PERGAMON
www.elsevier.com/locate/watres

PII: S0043-1354(00)00543-1

Wat. Res. Vol. 35, No. 10, pp. 2429–2434, 2001

Printed in Great Britain
0043-1354/01/$ - see front matter

AGGREGATION RATES OF NATURAL PARTICLE POPULATIONS

O. ATTEIA[1]*, C. MONDI[2] and D. PERRET[2]

[1]EGID, Universite Montaigne, 1 Allée F. Daguin, 33607 Pessac Cedex, France and [2]ICMA, UNIL, 1015 Lausanne, Switzerland

(First received 16 July 1999; accepted in revised form 13 October 2000)

Abstract—In this paper an experimental approach of aggregation in natural suspensions is presented. The suspensions are organic-matter-rich waters sampled in a brook which drains peat areas. The aggregation was conducted on raw samples in three different experiments lasting from 2 to 8 days. The particle size distribution (PSD) in the 0.5–10 μm size range was followed with a laser sizer and appeared to be almost constant along the whole experiment duration. Nevertheless, the volume of particles larger than 10 μm increased steadily, showing that aggregation occured. This appeared to be the consequence of a steady-state aggregation which allowed the removal of the whole particle set within a day. The use of an aggregation model adapted to calculations on PSD allowed estimation of the aggregation efficiency for such suspensions. © 2001 Elsevier Science Ltd. All rights reserved

Key words—aggregation, size distribution, river water, aggregation efficiency

INTRODUCTION

When addressing contaminant transport, colloids require specific attention because (i) they have a high surface area and reactivity, and (ii) their transport properties might differ from those of solutes. In groundwater, colloidal transport may differ in porous, fissured and karst aquifers. This is mainly due to the differences in the size of the void space, water velocities and ratio of water volume to sorption surfaces. In this paper we are dealing with karst aquifers and particularly with flow in large conduits, which might be compared to rivers. Due to the karst specific properties, the main phenomena influencing colloidal transport are sedimentation and aggregation. Sedimentation occurs in pools or lakes and is determined by the shear–stress distribution in the given structure (Hauns, 2000). Here we focus on the aggregation process which might play a significant role in particle settling. In the system that we are studying, as in most natural waters (McCarthy and Zachara, 1989; Perret *et al.*, 1994), the particles are often of very different nature and size. We, therefore, use the analysis of the whole particle size distribution (PSD) to characterise the aggregation process.

The experimental approach consisted in following the evolution of PSD during aggregation in the laboratory, completed by specific chemical analyses. On account of the extreme variety of natural particles characteristics, such as shape, density and chemical reactivity, the experimental results from natural suspensions are always scattered. Thus, only the major trends will be considered in the analysis of the following experimental results.

MATERIALS AND METHODS

For all experiments, natural water from a surface river sampled before its entrance into a karst network was used. The studied karstic basin, detailed previously (Atteia *et al.*, 1996), can be simplified as a flat valley of impervious sediments lying on calcareous rocks. The impervious sediments of the valley have led since the last glaciation to the development of large peat areas drained by small brooks. The waters used in the experiments came from one of these brooks and were taken under various hydrologic conditions. The chemical composition of the sampled waters are given in Table 1. The major characteristics are a high natural organic matter (NOM) content and a medium iron content. A lot of microscopic observations and analyses were done on the particles coming from this brook: they mostly consist of organo-mineral particles, clays and bacteria (Atteia *et al.*, 1998). The organo-mineral particles were analysed in detail and seem to be composed of a core of organic matter covered by iron (Couture *et al.*, 1998).

The experiments were conducted as follows. One litre of water was used for each treatment and put in a stirring bottle within 1 h from sampling. Then, the stirring velocity was fixed (~500 rpm) and never stopped until the end of the experiment. At each sampling time the PSD was analysed and 20 mL of each sample—100 mL for the last sample—was filtered in cascade to obtain raw, <10 μm, and <0.5 μm

*Author to whom all correspondence should be addressed. Tel.: +33-5-56-84-80-51; fax: +33-5-56-84-80-73; e-mails: atteia@egid.u-bordeaux.fr, didier.perret@icma.unil.ch

Table 1. Chemical composition of the waters used in the experiments: Fe^F is filtered (0.2 μm) iron and Fe^T is total iron

Experiment	pH	TOC $mg\,L^{-1}$	Ca $mg\,L^{-1}$	Mg $mg\,L^{-1}$	Fe^F $\mu g\,L^{-1}$	Fe^T $\mu g\,L^{-1}$	HCO_3^- $mg\,L^{-1}$	Cl^- $mg\,L^{-1}$	NO_3^- $mg\,L^{-1}$	SO_4^{2-} $mg\,L^{-1}$
1	6.95	25.0	81.1	3.1	373	847	59.2	2.4	2.5	5.4
2	7.25	35.4	82.7	4.49	878	2090	54.5	2.1	2.4	3.7
3	7.31	21.4	71	3.8	293	977	47.7	2.1	2.5	3.8

waters. For 10 μm cut-off we used Nylon filters (Millipore) and fibre glass ones for 0.5 μm (Nuclepore). A volume of 5 mL of each fraction was kept for iron analysis. The sampled volumes were small in order to keep the volume of the suspension as constant as possible. Unfortunately this does not allow a statistical analysis of the results.

PSD from 0.5 to 10 μm were analysed with a Galai CIS-I apparatus. This apparatus measures shadows of particles on a microscopic CCD detector and is, therefore, not influenced by particle nature (Jantschik *et al.*, 1992). Comparison with several other techniques revealed an error lower than 5% on cumulative distributions. However, measurements of particles larger than 20 μm were not reliable, certainly due to their small number and potential settling in the tubing (Atteia and Kozel, 1997). Pumping velocity was fixed at $50\,mL\,min^{-1}$ through a 6 mm side square cuvette, three replicate measurements were done and compared. For few samples, one replicate was rejected from the mean calculation if it was too different from the others. Due to the extreme differences in particle numbers of different size classes, the PSD have to be calculated using thick size classes for large particles and thin size classes for small ones. The only valid way to compare them is, therefore, to use the number or volume concentration of particles in each size class divided by the size of the class, i.e. in units of $L^{-1}\,m^{-1}$ or $m^3\,L^{-1}\,m^{-1}$ (O'Melia and Tiller, 1992). In this paper the volume fraction θ ($m^3\,L^{-1}$) is mostly used and the plots are presented in $d\theta/dd$ vs. d, where d is the particle size.

RESULTS AND DISCUSSION

The observed PSD evolution, shown in Fig. 1 for the three experiments, strikes one first by the stability of the PSD curves with time. In experiment 1, the PSD remains almost constant, in the range of the measurement error, during 50 h. The main difference between the first and last PSD is the volume increase in the >15 μm domain. Experiment 3 also shows constant PSD for small particles during 192 h; however, particles >10 μm, absent in the original sample appear during the experiment. Experiment 2 starting from a more concentrated suspension shows a decrease in particle volume for particles <10 μm, although the PSD shape remains constant. Volume fraction of particles larger than 25 μm increases during this experiment.

During the three experiments, variations in the particle volume in the 0.5–2 μm particle domain, higher than the measured standard deviation, can be observed. These variations are quite difficult to interpret as the particle volume in this size interval often decreases and then increases again.

The evolution of the PSD in the medium particle region gathered by summing up the particle volume in the 0.5–10 μm fraction—calculated from PSD measurements—is shown in Fig. 2. Presented as θ/θ_0, where θ_0 is the volume fraction at the beginning of the experiments, the results show a variation around the average value rather than a clear temporal trend. For experiments 1 and 3, the average ratio is close to 1, showing the stability of this volume fraction. In experiment 2 the volume fraction decreases at the beginning of the experiment and then remains almost stable.

Due to analytical difficulties, the mass of large particles was reliable only during the third experiment. These measurements are still approximate as they result from filtration of 20 mL followed by weighing of the filter. In experiment 3, the volume fraction of large particles (>10 μm) quickly becomes much more important than the volume fraction of the medium size range (0.5–10 μm) particles (Fig. 3(a)). The variations in the medium size range can be considered as secondary by comparison to the overall stability of the PSD. In fact the phenomenon (decrease and increase) is not monotonic and concerns negligible volumes (less than $0.1\,mm^3\,L^{-1}$) compared to volume fractions in the >10 μm size range.

Because matter is conserved, and as the 0.5–10 μm volume fraction remains almost stable, the only plausible explanation for the observed results is the occurrence of steady-state aggregation in the 0.5–10 μm range. In this size domain, each particle volume lost to larger size by aggregation is replaced by the same volume resulting from aggregation of smaller particles. The source of the increase of the volume fraction of large particles must then be found in the <0.5 μm fractions. The apparent result is a transfer of matter from the <0.5 μm fractions to the large particle fraction. Previous analyses of PSD, with another sizer or with SEM (Atteia and Kozel, 1997) showed that the observed Pareto distribution existed at least down to the 50 nm size in agreement with other measurements in groundwaters (Degueldre *et al.*, 1989). Very small particles are, therefore, present in a sufficient amount to let aggregation build 0.5 μm, or larger, particles. The increase of the volume fraction of large particles is thus due to the aggregation of smaller particles which are instantaneously replaced by smaller ones leading to the apparent paradox of the "birth" of particles ex nihilo.

Due to steady state, the aggregation rate, considered as the volume fraction passing from one size class to the next in one second, is thus constant for each class between 0.5 and 10 μm. It can then be calculated from the amount of particles passing the

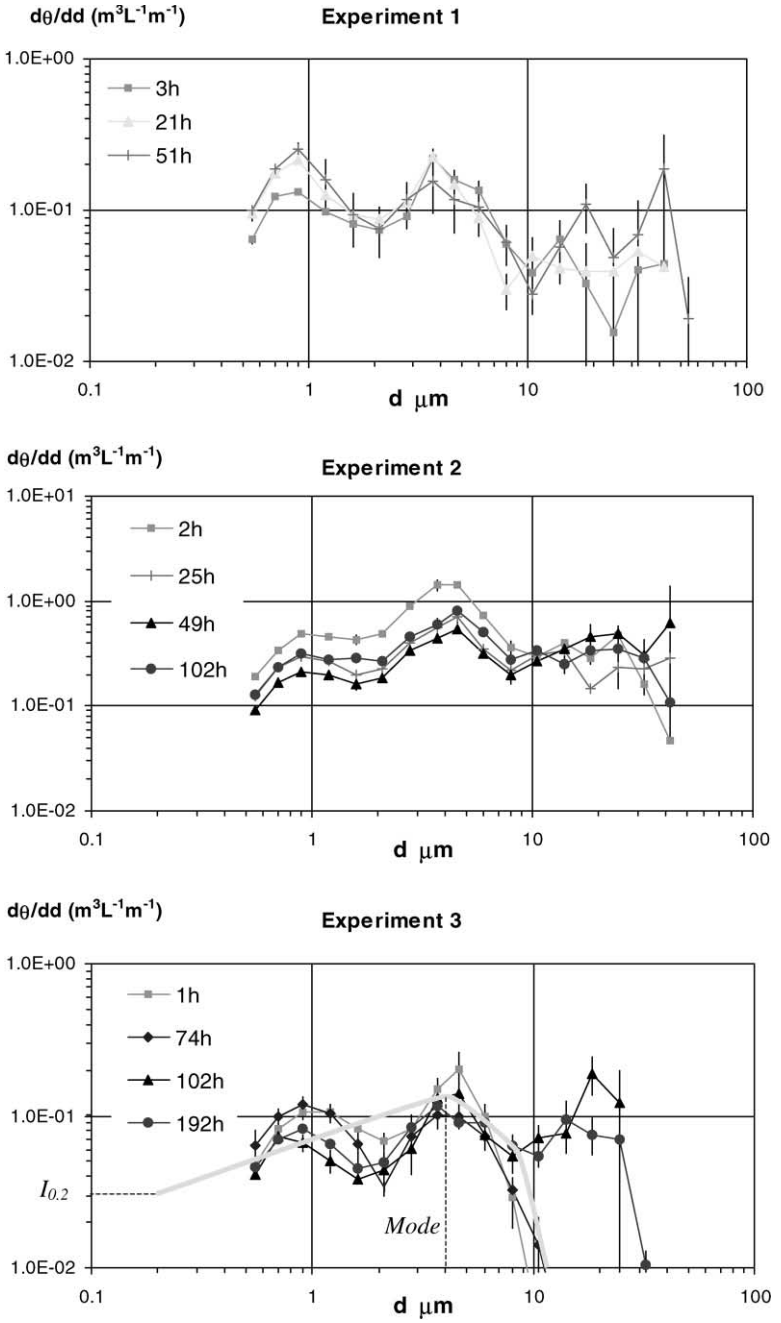

Fig. 1. Evolution of measured PSD during the three experiments, the *y*-axis is particle volume fraction divided by the size of the class. The height of the vertical bars represents the standard deviation for three replicates. Waters for experiments 1 and 3 were sampled at low flow and for experiment 2 at high flow. For experiment 3 the fitted steady-state PSD using parameters given in the text has been added (thick grey curve with no symbols). The modelled curve is not valid for diameters larger than 10 µm as it includes settling which is absent from the experiments.

10 µm size or the mass of the >10 µm particles obtained by filtration. These data are scattered due to the errors inherent to filtration for size determination (Buffle and Leppard, 1995). Figure 3(b) shows that the production rate of particles >10 µm is close to linear during the first 6 days, when measured on 20 mL samples. Higher values obtained for the last sample were more reliable as it used 100 mL of suspension. The average rate of production has been calculated by a linear fitting giving a weight twice higher to the last point, to account for the different sample size. This gives an approximate production rate of $2\,\mathrm{mg\,L^{-1}\,day^{-1}}$. This rate, compared to the volume of the <10 µm particle fraction, shows that all particles existing between 0.5 and 10 µm are replaced within a day: although similar PSDs are

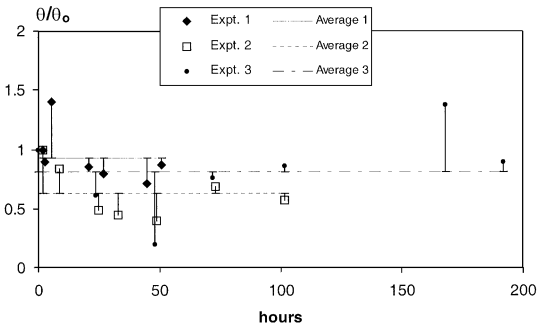

Fig. 2. Total volume of particles in the 0.5–10 μm range during the experiments, as calculated from the laser sizer data, expressed in θ/θ_0 where θ_0 is the inital volume fraction. Horizontal lines show the average value obtained from the whole experiment.

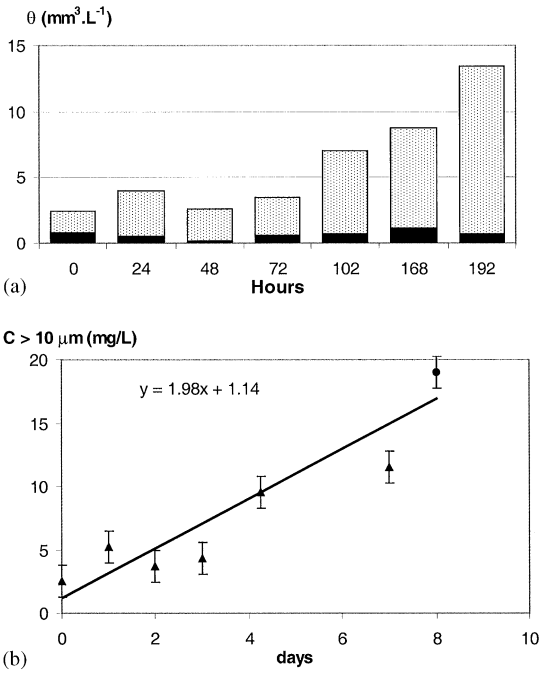

Fig. 3. Increase of mass of particles larger than 10 μm during experiment 3, obtained by filtration and weighting. In (a), the volume fraction of medium and large particles are compared. In (b), the line (and equation) is obtained by fitting the whole data set and giving a double weight to the last point, obtained on a 100 mL sample volume. The error bars correspond to an error of 25 μg as measured for the used balance.

measured each day, they do not consist of the same matter, such as the atoms of a living body that are replaced within a year.

Iron was measured in experiments 2 and 3. In experiment 2, the Fe content in the small particle fraction was obtained by sedimentation of the large particles and sampling of the supernatant. It showed a qualitative decrease during the experiment, which was detailed in experiment 3 using filtration. Figure 4 shows a slight decrease of Fe content in raw samples, a 50% reduction of Fe content of the $<10\,\mu m$ fraction and a 75% reduction in the $<1\,\mu m$ fraction. The total iron content of the suspension slowly decreases, while it should remain constant in a closed system. This can be attributed to the adsorption of particulate iron on the vessel and to the settling of large particles in the stirred vessel or in the sampling tube, particles which were, therefore, not analysed. Besides, the iron content is clearly transferred from the $<1\,\mu m$ fraction to the $>10\,\mu m$ fraction. This is the result of the aggregation process: the small particles containing iron are transformed into larger ones as explained above. In this closed system, the aggregation process generates particles which are gradually depleted from Fe. At the end of the experiment the particles should, therefore, consist mainly of organic matter, although this is difficult to verify by raw analytical chemistry due to the much larger amount of "dissolved" rather than particulate NOM.

We developed elsewhere (Atteia, 1998) an original aggregation model able to treat steady-state aggregation for PSD spanning several orders of magnitude in size range. This was done by adding, at a given rate θ_{add} ($m^3\,L^{-1}\,s^{-1}$) a volume fraction of small particles and leaving the system to equilibrate by aggregation, the removal of particles occurring by sedimentation. The input parameters are G, the shear rate in s^{-1}, $\alpha_{p,o}$ the aggregation efficiency for peri- and ortho-kinetic aggregation, f (%) the settling fraction according to hydraulic conditions and D the assumed fractal dimension of the aggregates. The simulated PSD, when presented in a $d\theta/dd$ vs. d plot, could easily be divided into three parts corresponding to Brownian aggregation, shear aggregation, and settling. The main characteristics of the curves, $I_{0.2}$ the intercept of the curve at 0.2 μm ($m^3\,L^{-1}$) and the Mode (m) were empirically related to the input parameters. We use here these relations as an "inverse modelling" to infer values of α_p and α_o from the "steady-state" PSD.

The following values were used for the physical parameters: a shear rate G of $10\,s^{-1}$ by comparison to literature experiments (Higashitani *et al.*, 1982;

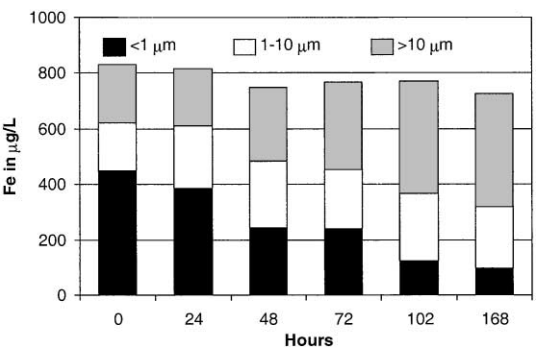

Fig. 4. Temporal evolution of iron content of the different size fractions obtained by filtration during experiment 3.

De Boer *et al*., 1989); a fractal dimension D of 2.5 as an estimated value from extrapolation of compact aggregates observations by microscopy and from literature (Elimelech *et al*., 1995); a θ_{add} value of $1.5 \times 10^{-14}\,m^3\,L^{-1}\,s^{-1}$ corresponding to the aggregation rate of $2\,mg\,L^{-1}\,day^{-1}$ calculated above; an intercept estimated from experimental curves as $I_{0.2} = 3 \times 10^{-2}\,m^3\,L^{-1}\,m^{-1}$. We used the following empirical relations detailed in the modelling paper:

$$I_{0.2} = \sqrt{\theta_{odd}/\alpha_p}, \tag{1a}$$

$$\text{Mode} = 4.36 \times 10^{-7} A_2^{-0.34}, \tag{1b}$$

with

$$A_2 = \frac{\alpha_o G}{50\alpha_p} e^{4(3-D)}, \tag{1c}$$

to calculate an estimated value of the aggregation efficiency for Brownian coagulation of $\alpha_p = 0.17$. This value is quite high but has been found in the literature (Filella and Buffle, 1993). This high aggregation efficiency could result from the high reactivity of Fe and NOM existing in these waters. The Mode of the distribution is close to 4 μm (4×10^{-6} m) which suggests, using the equations (1b) and (1c), a value of $\alpha_o = 1.7 \times 10^{-4}$ which, in that case, appears to be fairly small compared to α_p. However, in the literature concerning natural particles, the values of peri- and ortho-kinetic coagulation efficiencies are generally gathered in only one parameter and, therefore, do not allow for comparison. Besides, Zeichner and Schowalter (1977) described an experiment where the perikinetic aggregation becomes important only at very high shear rates ($400\,s^{-1}$) which can justify the secondary role of α_o in our experiments.

These extrapolations of α values are only qualitative because the measured PSD are much more scattered than the typical curves obtained by modelling. The mode of the distribution exists close to 4 μm, and the average slope of the curve between 0.5 μm and the Mode is close to 0.5 as predicted by the model. However it is clear from the measurements that the PSD between 0.5 and 4 μm does not fit to a power law (linear in log–log graph) as predicted; this part differs according to experiments and shows a hole close to 2 μm absent from the simulations. This suggests that the aggregation efficiency can differ with the size of the particle, or more probably with the particle type which for instance includes clays at size larger than 1 μm. A more detailed approach, using microscopy, should be done to differentiate the behaviour of each particle type during aggregation.

During runs 1 and 2, parallel experiments were conducted under nitrogen (therefore inhibiting aerobic bacterial growth). They do not show statistical difference with the ones opened to air. This suggests that the aggregation process is mostly chemically controlled and not biologically mediated.

CONCLUSION

Working on natural particles is a complex task due to the multiple particle types and the multi-disperse nature of the distributions. That is why our results are still approximate and the extrapolated values of aggregation efficiencies α might be considered as estimates. However the main result of the experiments is clear: the sampled PSD are at steady state with respect to aggregation. This statement has several important general consequences: (i) the aggregation rate is almost constant in the range 0.5–10 μm and can be measured at one specific size, (ii) the shape of the PSD in natural suspensions appear to result mostly from aggregation, and, (iii) a complete renewal of the particles occurs during a day in the measured size range. This last point may have important implications on the transport of particulate matter: the contaminants associated with small particles will accumulate in larger particles and settle within few days. This could explain why, in the considered karstic aquifer, iron associated with 0.2–0.5 μm particle, is not recovered at the outlet after a transit of several days in the aquifer.

Acknowledgements—This research has been funded by the Swiss National Science Foundation, PACT project (FN 21-043 438.95).

REFERENCES

Atteia O. (1998) Evolution of size distributions of natural particles during aggregation: modelling versus field results. *Colloid. Surf. A* **139**, 171–188.

Atteia O., Gogniat S. and Kozel R. (1996) Apport de l'hydrogéologie de la géophysique et des essais de traçage à la connaissance de l'aquifère karstique de la Noiraigue Jura neuchâtelois, Suisse. *Bull. Hydrogéol. Univ. Neuchâtel Suisse* **15**, 33–61.

Atteia O. and Kozel R. (1997) Particle size distributions in waters from a karstic aquifer: from particles to colloids. *J. Hydrol.* **201**, 102–119.

Atteia O., Perret D., Adatte T., Kozel R. and Rossi P. (1998) Characterization of natural colloids from a karstic aquifer. *Environ. Geol.* **34/4**, 257–269.

Buffle J. and Leppard G. G. (1995) Characterization of aquatic colloids and macromolecules. 1. Structure and behaviour of colloidal material. *Environ. Sci. Technol.* **29/9**, 2169–2175.

Couture C., Mavrocordatos D., Atteia O. and Perret D. (1998) The genesis and transformation of organo-mineral colloids in a drained peatland area. *Phys. Chem. Earth* **23**(2), 153–157.

De Boer G. B. J., Hoedemakers G. F. M. and Thoenes D. (1989) Coagulation in turbulent flow: Part I. *Chem. Engng. Res. Des.* **67**, 301–307.

Degueldre C., Baeyens B., Goerlich W., Riga J., Verbist J. and Stadelmann P. (1989) Colloids in water from a subsurface fracture in granitic rock, Grimsel Test Site, Switzerland. *Geochim. Cosmochim. Acta* **53**, 603–610.

Elimelech M., Gregory J., Jia X. and Williams R. (1995) *Particle deposition and aggregation, Measurement modelling and simulation*. Butterworths-Heinemann, London.

Filella M. and Buffle J. (1993) Factors controlling the stability of submicron colloids in natural waters. *Colloid. Surf. A* **73**, 255–273.

Hauns M. (2000) Modeling tracer and particle transport in karst conduit structures. Ph.D. Thesis, University of Neuchatel, Suisse.

Higashitani K., Ogawa R., Hosokawa G. and Matsuno Y. (1982) Kinetic theory of shear coagulation for particles in a viscous fluid. *J. Chem. Engng. Japan* **15**, 299–304.

Jantschik R., Nyffeler F. and Donard O. F. X. (1992) Marine particle size measurement with a stream-scanning laser system. *Marine. Geol.* **106**, 239–250.

McCarthy J. F. and Zachara J. M. (1989) Subsurface transport of contaminants. *Environ. Sci. Technol.* **23**, 496–502.

O'Melia C. R. and Tiller C. L. (1992) *Physico-chemical aggregation and deposition in aquatic environments*, Environmental particles volume I, IUPAC Series on environmental analytical and physical chemistry, pp. 353–386. Lewis Publisher, Chelsea, MI.

Perret D., Newman M. E., Nègre J. -C., Chen Y. and Buffle J. (1994) Submicron particles in the Rhine river–I, Physico-chemical characterization. *Water Res.* **28**, 91–106.

Zeichner G. R. and Schowalter W. R. (1977) Use of trajectory analysis to study stability of colloidal dispersions in flow fields. *A.I.Ch.E.J.* **23**, 243–254.